Measured Aerodynamic Interaction of Two Tiltrotors

Gloria K. Yamauchi
Gloria.K.Yamauchi@nasa.gov
Aerospace Engineer
NASA Ames Research Center
Moffett Field, CA, USA

Alan J. Wadcock
awadcock@mail.arc.nasa.gov
Principal Scientist
Aerospace Computing, Inc.
Moffett Field, CA, USA

Michael R. Derby
mderby@mail.arc.nasa.gov
Principal Engineer
Aerospace Computing, Inc.
Moffett Field, CA, USA

Abstract

The aerodynamic interaction of two model tiltrotors in helicopter-mode formation flight is investigated. Three scenarios representing tandem level flight, tandem operations near the ground, and a single tiltrotor operating above the ground for varying winds are examined. The effect of aircraft separation distance on the thrust and rolling moment of the trailing aircraft with and without the presence of a ground plane are quantified. Without a ground plane, the downwind aircraft experiences a peak rolling moment when the right (left) rotor of the upwind aircraft is laterally aligned with the left (right) rotor of the downwind aircraft. The presence of the ground plane causes the peak rolling moment on the downwind aircraft to occur when the upwind aircraft is further outboard of the downwind aircraft. Ground plane surface flow visualization images obtained using tufts and oil are used to understand mutual interaction between the two aircraft. These data provide guidance in determining tiltrotor flight formations which minimize disturbance to the trailing aircraft.

Notation

A	rotor disk area, πR^2
C_{Mx}	aircraft roll moment coefficient, $M_x /(\rho(\Omega R)^2 AR)$, positive right wing down
C_T	aircraft thrust coefficient, aircraft thrust/$(2\rho(\Omega R)^2 A)$
D	rotor diameter
DW	downwind
M_{tip}	blade tip Mach number, ΩR /sound speed
M_x	aircraft roll moment
R	rotor blade radius
s	wing semispan
UW	upwind
x	streamwise location of UW aircraft relative to DW aircraft, positive in drag direction
y	lateral location of UW aircraft relative to DW aircraft, positive to right (pilot's view)
z	vertical location of UW aircraft relative to DW aircraft, positive up
μ	advance ratio, tunnel speed/ΩR
Ω	rotor rotational speed
ρ	air density
σ	rotor solidity

Presented at the American Helicopter Society 59th Annual Forum, Phoenix, Arizona, May 6-8, 2003.

Introduction

Vertical take-off or landing runway independent aircraft (VTOL RIA) have the potential to significantly alleviate air space congestion. Tiltrotors are a primary example of VTOL RIA. A key element of air space management is to understand how these aircraft behave near other aircraft, near large structures such as buildings, and near the ground. For each of the aforementioned scenarios, the aerodynamic interactions are complex. In order to establish guidelines for safe operation of VTOL RIA near other objects, experimental data quantifying these interactions are required.

The Army/NASA Rotorcraft Division at NASA Ames Research Center has initiated an experimental program addressing the aerodynamic interaction between VTOL RIA in terminal area operation scenarios. This paper presents measurements from a wind tunnel test of two model tiltrotors. The test was conducted in the Army 7- by 10-Foot Wind Tunnel at NASA Ames Research Center. Models roughly approximating 1/48th-scale V-22 rotors and wing were used for the experiment. Details of vortex formation are not expected to be captured at 1/48th-scale; however, the aerodynamic interactions should be representative of full-scale results based on previous work at low Reynolds number. For example, Ref. 1 investigated tiltrotor descent aerodynamics using a model only slightly larger than the models in the present experiment and found reasonable agreement with results from a similar test conducted at a larger scale (Ref. 2). Based on the calculations of Ref. 3, at some distance downstream the tiltrotor wake is known to resemble the wake of a fixed wing aircraft. The parameters that

govern the strength and position of the trailed wake are rotor thrust and forward speed, not details of the rotor geometry. If key nondimensional parameters such as rotor thrust coefficient and advance ratio can be matched between model and full-scale results, the model scale data should provide a good representation of full-scale events.

This paper provides quantitative measurements of the aerodynamic interaction of two tiltrotors operating in helicopter mode. The interaction is presented in terms of rolling moment and thrust changes on the downwind aircraft. Three scenarios are examined. The first scenario represents two tiltrotors in level flight. The second scenario, using a ground plane, has the downwind aircraft at reduced thrust with wheels on ground while the upwind aircraft is in descent (or take-off). The two aircraft are also tested without the ground plane to assess the changes in the interaction between the two aircraft that are directly due to the presence of the ground plane. Ground plane surface flow visualization images obtained using tufts and oil are also shown. Finally, a single tiltrotor is tested at various heights above the ground for several wind speeds.

Facility and Model Description

The 7-by 10-Foot Wind Tunnel is a closed circuit wind tunnel operated by the U.S. Army Aeroflightdynamics Directorate at NASA Ames Research Center. The test section is 7-ft high, 10-ft wide and 15-ft long. The tunnel has a 14:1 contraction ratio providing a maximum speed of approximately 355 ft/s. The test section turntable is capable of yaw angles up to 360 degrees. An air exchange system allows up to 29.3% air exchange. Since target speeds for this experiment ranged from 13 to 26 ft/s, the tunnel was run with 0% air exchange to eliminate atmospheric influence on the test section flow steadiness. A traverse system, installed in the test section, is capable of traversing in the vertical, lateral, and streamwise directions.

The tiltrotor models were designed and built at NASA Ames. Characteristics of the model are provided in Table 1. Key characteristics of the geometry such as rotor planform, twist distribution, and lateral rotor-rotor spacing are similar to a 1/48th-scale V-22. The blades, however, were fabricated with a blade radius closer to a 1/49th-scale V-22 rotor. Figure 1 is an assembly drawing showing the model component parts. For this experiment, a fuselage was not modeled since the primary aerodynamic interaction between the aircraft was assumed to be dominated by the rotors. The three-bladed hubs have counter-clockwise rotation on the right rotor and clockwise rotation on the left rotor. The wing is machined aluminum with zero flap deflection. The hub and control systems are commercially available radio-control model helicopter tail-rotor assemblies. The rotors have collective pitch control allowing trim of aircraft thrust and rolling moment. The rotors do not have flap or lag hinges, or a gimbal, and do not have cyclic pitch control. Hence, the rotors operate with some hub moment in helicopter mode forward flight. An Astro Cobalt-40 sport motor mounted in the nose of each aircraft is used to power the rotors. Each aircraft was mounted on a 6-component, 0.75-inch balance.

The design tip speed (263 ft/s) of the rotors is approximately 1/3 full-scale, corresponding to a rotor rpm of 6355. The Reynolds number based on blade tip chord and speed is approximately 63,000. Additional details of the model design are reported in Ref. 4.

Table 1. Model Aircraft Characteristics

No. of rotors (3 blades each)	2
Rotor radius, R (ft)	0.3906
Blade tip chord (ft)	0.0372
Rotor-rotor separation distance, 2s (ft)	0.9703
Root cut-out (%)	25.5
Rotor solidity, σ	0.102
Wing flap setting (deg)	0
Nacelle angle (deg)	90
Target rotor rpm, Ω	6355
Target tip speed ΩR (ft/s)	263

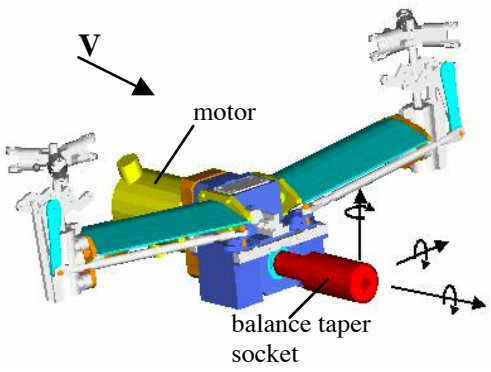

Figure 1. CAD model of tiltrotor.

Experimental Set-Up

The downwind aircraft was mounted on a fixed pedestal sting. The upwind aircraft was sting-mounted and suspended from a streamlined strut attached to the tunnel traverse system. The pitch of both aircraft was fixed at zero, therefore, the rotor tip-path planes were both parallel to the freestream. The upwind model was traversed in the lateral, vertical, and streamwise directions upstream of the downwind aircraft. Data were acquired without and with the presence of a ground

plane. The ground plane is 4-ft by 8-ft and approximately 1.25 inches thick with a rounded leading edge. Figures 2a) and 2b) show the two aircraft mounted in the wind tunnel without and with the ground plane, respectively. Figure 3 is a sketch showing the fixed position of the downwind aircraft with respect to the ground plane and some of the key positions of the upwind aircraft in the x-y plane.

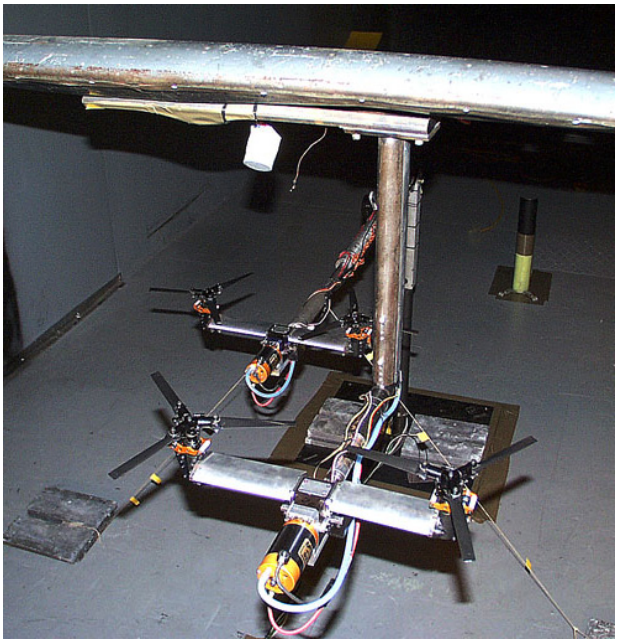

a) Without ground plane.

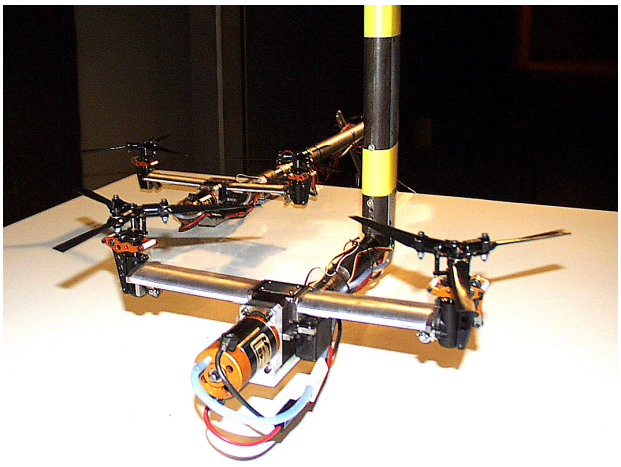

b) With ground plane.

Figure 2. Installation of two tiltrotors in the U. S. Army 7- by 10-Foot Wind Tunnel.

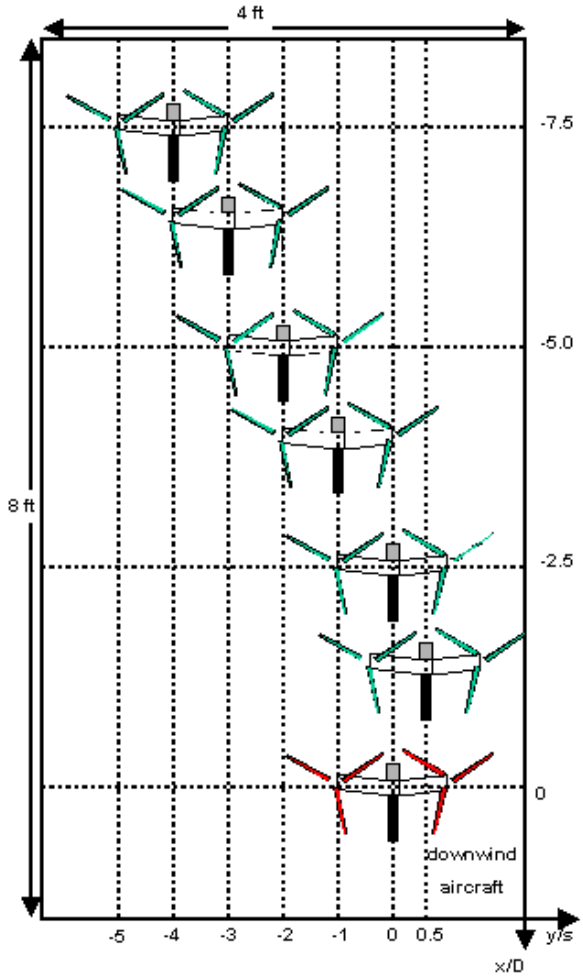

Figure 3. Relative aircraft positions with ground plane installed (approximate scale, top view). Wind from top to bottom.

Testing Procedure

With the downwind aircraft in a fixed position, the upwind aircraft was traversed in the cross-flow plane at various streamwise locations. Primary streamwise locations were x/D=-2.54, -5.08, -7.62, and -10.16 (approximated as -2.5, -5, -7.5, and -10 when describing the figures in this paper). The thrust and roll moment of the downwind aircraft were the primary measurements of the aerodynamic interaction between the two aircraft. To establish a reference condition for the downwind aircraft, the following procedure was used. The upwind aircraft, with rotors stationary, was positioned upstream at the traverse extreme upper left (pilot's view). The downwind model rpm was then increased to the design value at low thrust. Wind tunnel speed was then increased from zero to the desired advance ratio. Next, the downwind aircraft was trimmed to the desired thrust coefficient and the rolling moment was trimmed to approximately zero (using differential collective pitch

control) thus establishing a wind-on reference condition without the influence of the upwind aircraft. From this point on, the controls of the downwind aircraft were fixed, so the aircraft trim was free to vary. The upwind aircraft rotor speed was then increased from zero to the design speed and the aircraft was moved into position to commence traversing in a cross-flow (y-z) plane. The upwind aircraft was trimmed to the target thrust coefficient and approximately zero rolling moment for each data point. Trimming was normally only necessary when the aircraft was moved in and out of ground effect. In addition to cross-flow plane surveys, height sweeps at specific y/s and x/D were also performed.

Results

Three VTOL RIA scenarios are examined for tiltrotors in helicopter-mode flight. The first scenario simulates two tiltrotors in level flight. Rolling moment and changes in thrust on the downwind aircraft as a function of upwind aircraft position are presented. The effect of advance ratio on the downwind aircraft rolling moment and thrust, and the effect of upwind aircraft thrust on downwind aircraft rolling moment are discussed. Rolling moment is related to full-scale aircraft differential collective pitch using existing isolated tiltrotor data. The second scenario examines operations near the ground. Using a ground plane, the downwind aircraft is established at reduced thrust with wheels on the ground while the upwind aircraft is in descent (or take-off). The two aircraft are also tested without the ground plane to assess the changes in the interaction between the two aircraft due directly to the ground plane. All force and moment data presented are relative to the wind-on reference condition described previously. Flow visualization using ground plane surface oil patterns and tuft patterns are shown. The third scenario simulates a single tiltrotor operating at various heights above the ground with varying winds. Resulting changes in thrust are presented. Table 2 lists the specific test conditions explored during the experiment.

Table 2. Test Conditions

Scenario	Run	M_{tip}	μ	DW A/C	UW A/C				Ground plane
				C_T/σ initial	C_T/σ	x/D	y/ s	z/s	
1	122 123 126	0.23	0.10	0.121 0.120 0.122	0.121 0.121 0.120	-2.5 -5.0 -10.0	traverse		No
1	127	0.23	0.10	0.122	0.090	-2.5 -5.0 -7.5 -10.0	-2	vary	No
1	128	0.23	0.05	0.122	0.121	-2.5 -5.0 -7.5 -10.0	-2	vary	No
1	129	0.23	0.05	0.122	0.090	-2.5 -5.0 -7.5 -10.0	-2	vary	No
2	142 143 145	0.23	0.10	0.018 0.018 0.018	0.120 0.120 0.120	-2.5 -5.0 -7.5	traverse		Yes
2	150	0.23	0.10	0.019	0.120	-2.5	-2.5	1	Yes (with oil)
2	152	0.23	0.10	0.018	0.120	vary	vary	vary	Yes (with tufts)
3	155	0.23	0 0.05 0.10	N/A	0.120 initial	-5.0	-1.7	vary	Yes
2	169 170 174	0.23	0.10	0.018 0.018 0.019	0.121 0.121 0.121	-2.5 -5.0 -7.5	traverse		No

Scenario 1: Level Flight

For the level flight condition investigated, the downwind aircraft initial C_T/σ was about 0.12. The upwind aircraft C_T/σ was maintained at approximately 0.12. Figures 4a and 4b show the rolling moment (C_{Mx}/σ) and thrust change ($\Delta C_T/\sigma$), respectively, of the downwind aircraft as a function of upwind aircraft position in the y-z plane at x/D=-2.5 for advance ratio=0.10. These results were presented in Ref. 3 and are shown here again to explain certain features of the data. Measurements were acquired at the grid points indicated on the plots. Note that the rolling moment data in Fig. 4a are anti-symmetrical about y/s=0 providing confidence in the quality of the data. Reference 3 used the comprehensive rotorcraft analysis CAMRAD II to calculate rolling moment on the trailed aircraft as a function of the lead aircraft position. The correlation between the calculations and measurements from this test was good.

The data clearly show peak rolling moments at y/s=±2 corresponding to the right (left) rotor of the upwind aircraft being aligned laterally with the left (right) rotor of the downwind aircraft (see Fig. 3). Note that a right roll (pilot's view) is defined as positive. At y/s=-2, the left rotor of the downwind aircraft is in the downwash of the upwind right rotor thus causing a thrust reduction on the left downwind rotor resulting in a negative roll. At y/s=2, the opposite situation occurs. Figure 4b shows the change in thrust on the downwind aircraft relative to the wind-on reference condition. There is a significant reduction in thrust when the two aircraft are aligned laterally (y/s=0) at z/s=1. The slight increase in thrust at y/s=-4 and z/s=1 corresponds to a positive rolling moment suggesting a thrust increase on the left rotor compared to the right rotor of the downwind aircraft.

Reference 3 shows that the magnitudes and lateral location of the peak roll moment and thrust change do not change significantly as x/D was varied from -2.5 to -10. In addition, Ref. 3 calculated the change in power required to trim the downwind aircraft for the conditions corresponding to Fig. 4. At the location (y/s=-4, z/s=1) of the thrust increase in Fig. 4b, a reduction in power required is predicted. Although optimizing formation spacing to maximize the downwind aircraft performance was not the intent of this study, especially since aircraft power was not measured, future experiments with these tiltrotor models can be designed with this objective in mind. References 5-7 provide both analytical and experimental confirmation of the benefits of flying airplanes in an echelon formation. Similar benefits should be applicable to tiltrotors and helicopters.

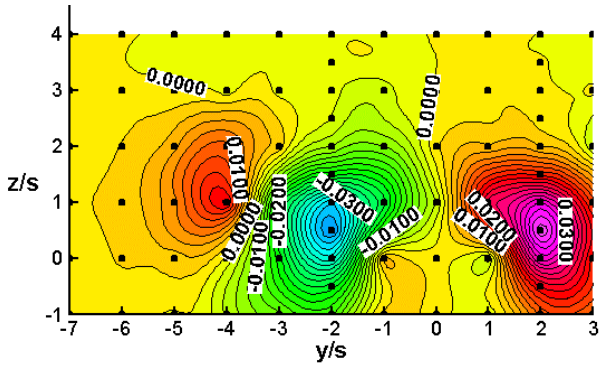

a) C_{Mx}/σ

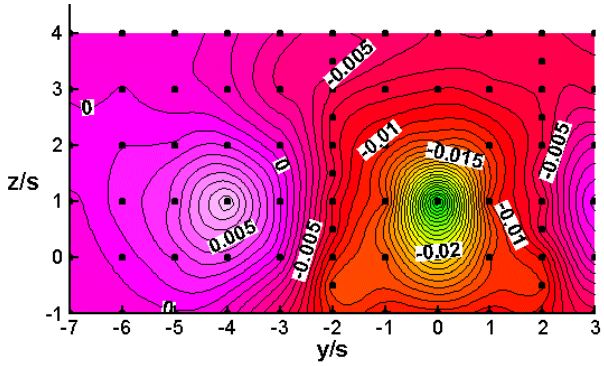

b) $\Delta C_T/\sigma$

Figure 4. Run 122: Rolling moment and thrust change on DW aircraft as a function of UW aircraft position. x/D=-2.5. Advance ratio=0.10. DW C_T/σ (initial)=0.12; UW C_T/σ=0.12.

Effects of advance ratio and upwind aircraft thrust on the downwind aircraft rolling moment were explored by performing upwind aircraft streamwise and height surveys at y/s=-2, corresponding to the peak negative rolling moment location of Fig. 4a. Figure 5 shows the peak C_{Mx}/σ decreases only slightly as the upwind aircraft moves from x/D=-2.5 to -10. Since the wake skew angle of the upwind aircraft is maintained (C_T and μ of the aircraft are held constant), the upwind aircraft height must increase with increasing x/D in order for the upwind aircraft rotor wakes to interfere at the same location on the downwind aircraft. The measured vertical shift of the peak from x/D=-2.5 to -10 implies a wake skew angle of approximately 5 degrees.

The effect of reducing advance ratio from 0.10 to 0.05 is shown by comparing Fig. 5 with Fig. 6. As in Fig. 5, the downwind aircraft initial C_T/σ was about 0.12 and the upwind aircraft C_T/σ was maintained at 0.12. Figure 6 shows the magnitude of the peak roll moment is essentially unchanged from the μ=0.10 case

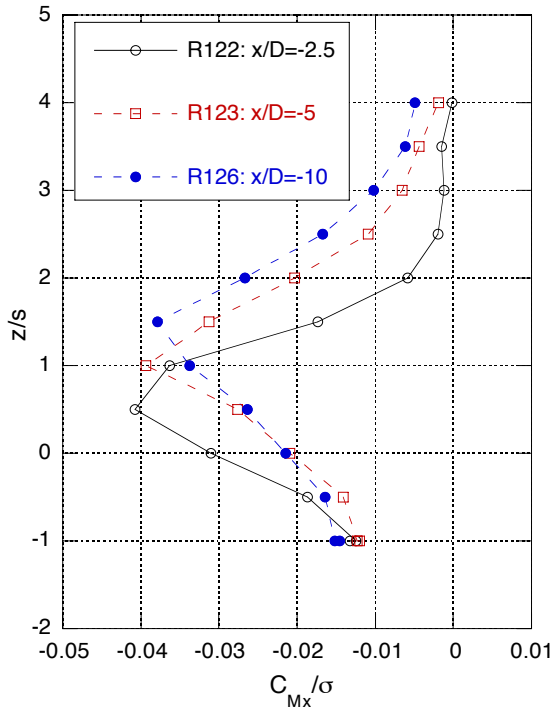

Figure 5. Effect of UW aircraft vertical sweep (at y/s=-2) on DW aircraft C_{Mx}/σ. Advance ratio=0.10. DW C_T/σ (initial)=0.12; UW C_T/σ=0.12.

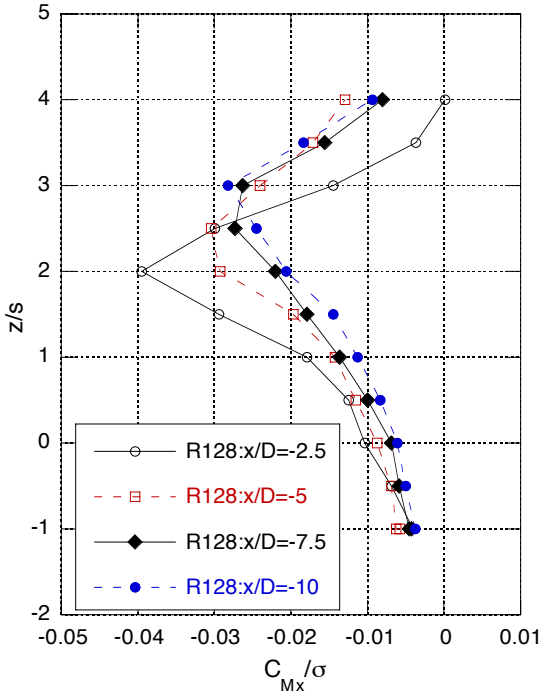

Figure 6. Effect of UW aircraft vertical sweep (at y/s=-2) on DW aircraft C_{Mx}/σ. Advance ratio=0.05. DW C_T/σ (initial)=0.12; UW C_T/σ=0.12.

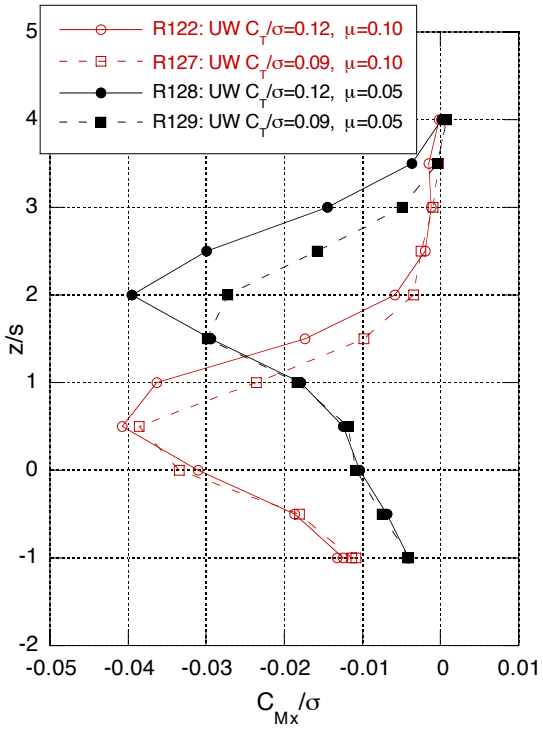

Figure 7. Effect of advance ratio and upwind aircraft C_T/σ on DW aircraft C_{Mx}/σ. UW aircraft vertical sweep at y/s=-2, x/D=-2.5. DW C_T/σ (initial)=0.12.

at x/D=-2.5 but has decreased at the larger x/D locations. At μ=0.05, the wake skew angle is larger as evidenced by the peak occurring at increased z/s compared to Fig. 5. Since the magnitude of the peak roll moment is largest at x/D=-2.5, we next examine the effect of reducing the upwind aircraft thrust at this streamwise location. Figure 7 shows there is little effect on the peak roll moment magnitude when the upwind aircraft C_T/σ is reduced from 0.12 to 0.09 at μ=0.10. At μ=0.05, however, there is a reduction in the peak roll moment of about 25% when the C_T/σ is reduced.

Estimating Differential Collective Pitch

Inferring the differential collective pitch required to trim the measured rolling moment on the downwind aircraft provides useful information applicable to full-scale formation flight. Although the models had collective and differential collective pitch control, a relationship between thrust and collective was not obtained because of hysteresis in the control system. This was not a problem since test conditions targeted specific C_T values rather than collective pitch. However, an estimate of the differential collective pitch required to trim the rolling moment can be derived. The rolling moment is assumed to be caused solely by the differential thrust between the left and right rotors and

the wing contribution to rolling moment is assumed negligible. Hence,

$M_x = s(\Delta T)$, where $\Delta T = T_{left} - T_{right}$

or

$(R/s)(C_{Mx}/\sigma) = \Delta(C_{\Delta T}/\sigma)$.

Note that $C_{\Delta T}$, the change in thrust between two rotors, is defined as $\Delta T/\rho A(\Omega R)^2$ which is different than the definition of aircraft C_T. Next, a relationship between $\Delta(C_{\Delta T}/\sigma)$ and $\Delta\theta$ is needed. Table 3 provides values for $\Delta(C_{T\_iso}/\sigma)/\Delta\theta$ taken from several isolated tiltrotor databases (Refs. 2, 8-12). Values are provided for $0.05 \le C_{T\_iso}/\sigma \le 0.15$, which bounds the C_T/σ range for the downwind aircraft in Figs. 4-7. Data from Refs. 2 and 11 indicate the value of $\Delta(C_{T\_iso}/\sigma)/\Delta\theta$ does not change appreciably with advance ratio. For a peak C_{Mx}/σ of 0.04 shown in Fig. 4a and using a value of $\Delta(C_{\Delta T}/\sigma)/\Delta\theta = \Delta(C_{T\_iso}/\sigma)/\Delta\theta = 0.54$ (representing the average of the values in Table 3), a $\Delta\theta$ of 3.4 deg or ±1.7 deg per rotor is obtained. Using CAMRAD II, Ref. 3 calculates approximately ±2 deg of differential collective pitch for the equivalent C_{Mx}/σ, which is consistent with the level calculated here.

Table 3. Isolated Tiltrotor Thrust Derivative

Experiment	$\Delta(C_{T\_iso}/\sigma)/\Delta\Theta$, rad^{-1}, for $0.05 < C_{T\_iso}/\sigma < 0.15$
JVX/OARF (Ref. 8)	0.5307
XV-15/OARF (Ref. 9)	0.5880
XV-15/80x120 (Ref. 10)	0.5777
TRAM/DNW (Ref. 11)	
μ=0	0.5182
μ =0.15	0.4681
μ =0.175	0.5017
μ =0.20	0.5088
4 ft diam. tiltrotor/80x120 (Ref. 2)	
μ=0	0.6055
μ =0.04	0.5734
μ =0.10	0.5457
μ =0.12	0.5958
4 ft diam. tiltrotor/hover chamber (Ref. 12)	0.5176

Scenario 2: Tandem Operations Near the Ground

A likely scenario for terminal area operations has one tiltrotor positioned on a landing pad at low thrust while another tiltrotor is positioned upwind and above (representing either descent or take-off). This scenario was simulated by installing a ground plane beneath both aircraft (Figs. 2b and 3). Since the ground plane was only 4-ft wide by 8-ft long, the separation distance between the aircraft was limited to $-7.5 \le x/D \le -2.5$ and $-4 \le y/s \le 0.5$. From the wake calculations of Ref. 3 and from preliminary velocity field measurements behind the upstream tiltrotor, the eventual formation of two super-vortices is confirmed at approximately x/D= -2 to -2.5. A tiltrotor wake looks very much like the wake of a fixed wing aircraft. Each rotor disk is assumed to shed a counter-rotating vortex pair. Vortices shed from the inboard side of each disk are equal in magnitude but opposite in sign leading to vortex cancellation because of their close proximity. The outboard vortex from each disk remains to dominate the far wake as super-vortices. When these super-vortices approach the ground plane, they tend to migrate outward since the ground plane acts as an image plane.

Figures 8 and 9 show contours of the downwind aircraft rolling moment as a function of upwind aircraft position with and without the ground plane, respectively, for several aircraft separation distances. The initial C_T/σ of the downwind aircraft was 0.018 and the upwind aircraft was trimmed to about C_T/σ=0.12 and approximately zero roll moment. The locations where data were acquired are shown as overlaid grid points. With the ground plane present, the lowest vertical position of the upwind aircraft was limited to z/s values slightly greater than zero to prevent wiring and cooling lines which hang below the aircraft from touching the ground plane. Data without the ground plane (Fig. 9) are shown solely to illustrate the effects of the ground plane – the low C_T/σ of the downwind aircraft is unrealistic for level flight. With the ground plane present, the peak negative roll moment location moves outboard as x/D is varied from -2.5 to -7.5. The magnitude of the peak negative moment is somewhat mitigated by the ground plane. Interestingly, a positive peak moment is present at y/s=-1 with the ground plane. This peak positive moment is possibly caused by the super-vortex from the right upwind rotor that, instead of traveling straight downstream, has moved outward to the right under the influence of the ground plane. This causes the right downwind rotor to be in a downwash and impart a positive roll to the downwind aircraft. Without the ground plane, the lateral location of the peak rolling moment and thrust do not change with increasing separation distance indicating that the wake from the upwind aircraft convects straight downstream.

Figures 10 and 11 show contours of the downwind aircraft change in C_T/σ from the reference value (C_T/σ =0.018) for conditions similar to Figs. 8 and 9. There is a peak thrust deficit on the downwind aircraft at y/s=0 and z/s=1. The presence of the ground plane reduces the level of the thrust deficit for all x/D examined. The levels are still large, however, compared to the reference C_T/σ value of 0.018. In the presence of the ground plane, the peak moves increasingly outward laterally as

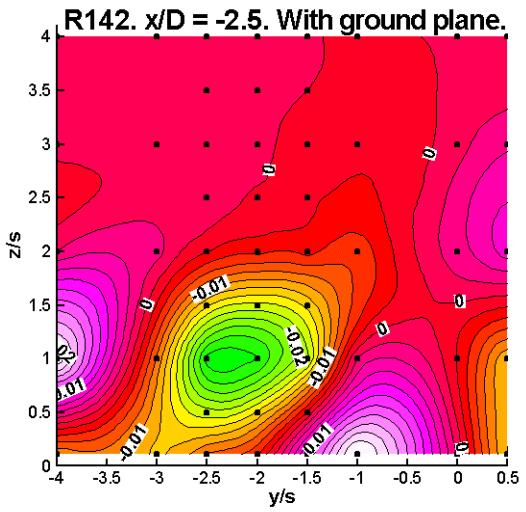

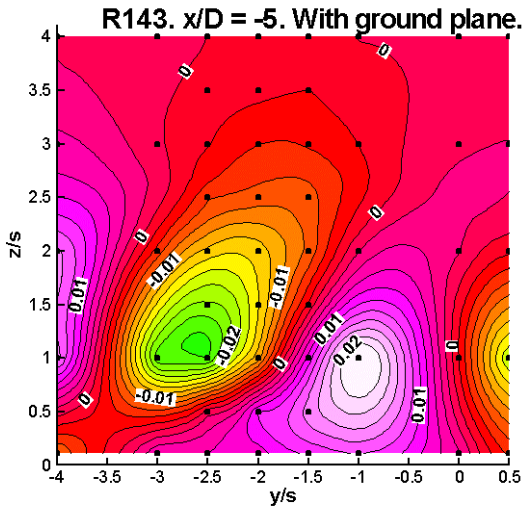

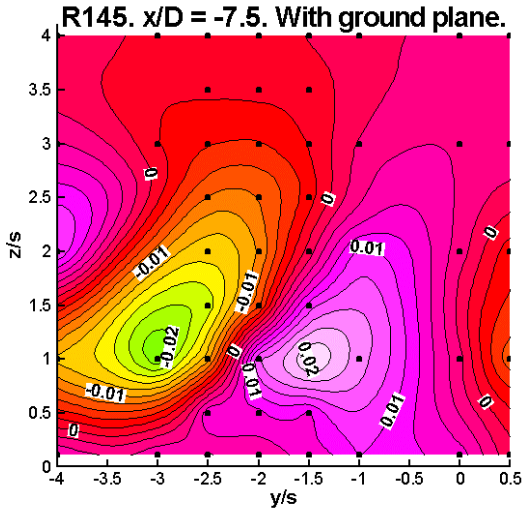

Figure 8. DW aircraft C_{Mx}/σ as a function of UW aircraft position. With ground plane. μ =0.10. DW C_T/σ (initial)=0.018; UW C_T/σ=0.12.

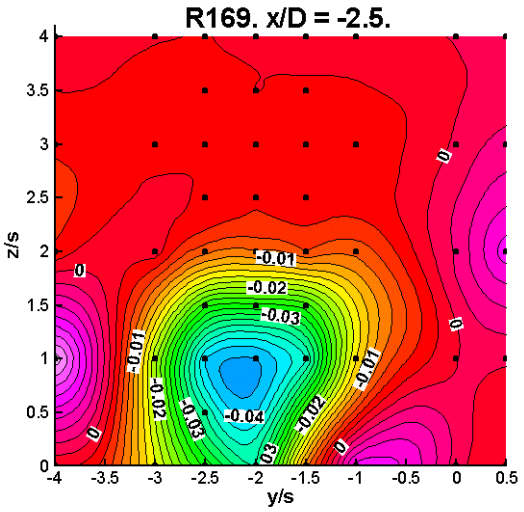

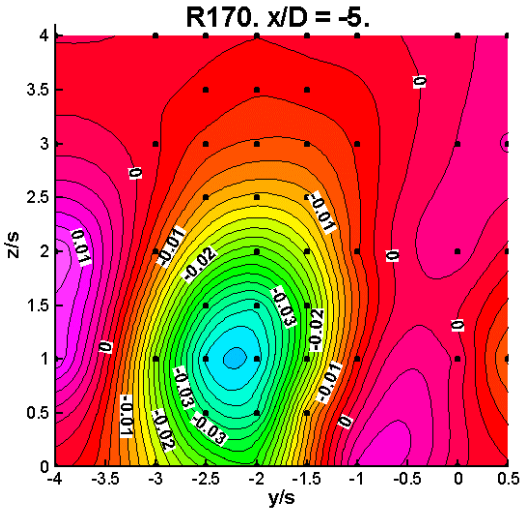

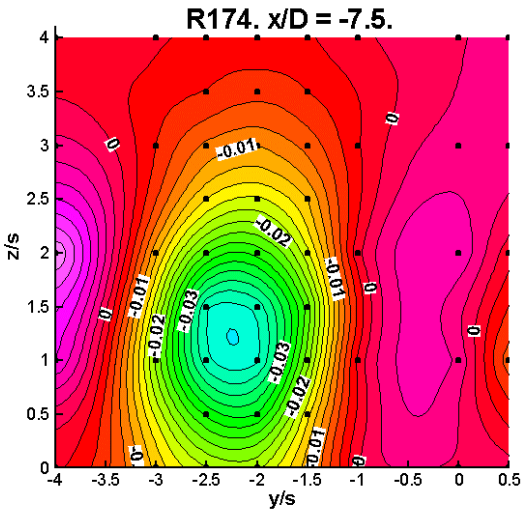

Figure 9. DW aircraft C_{Mx}/σ as a function of UW aircraft position. Without ground plane. μ =0.10. DW C_T/σ (initial)=0.018; UW C_T/σ=0.12.

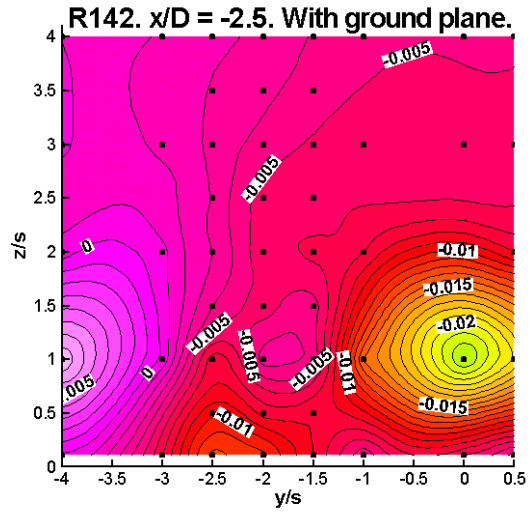

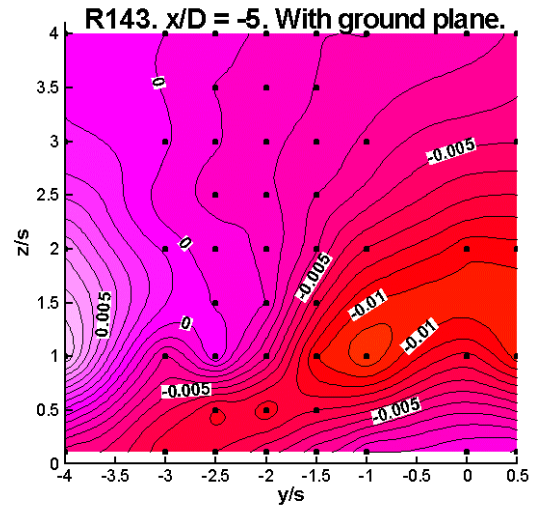

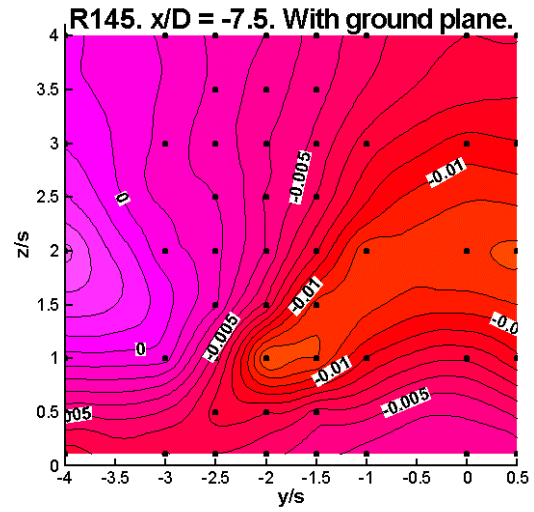

Figure 10. DW aircraft $\Delta C_T/\sigma$ as a function of UW aircraft position. With ground plane. μ =0.10. DW C_T/σ (initial)=0.018; UW C_T/σ=0.12.

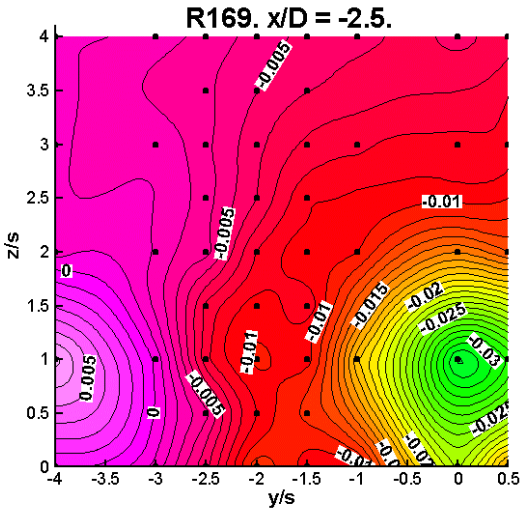

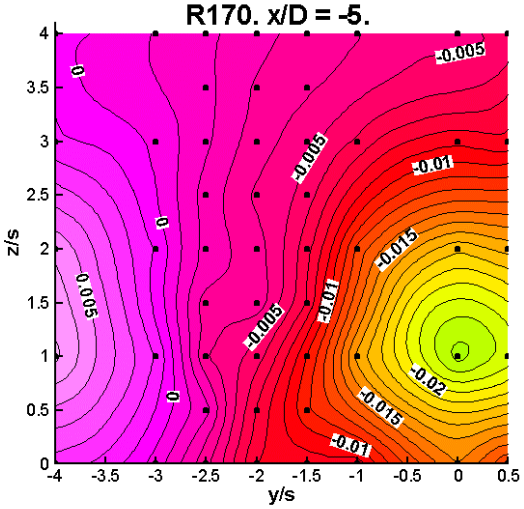

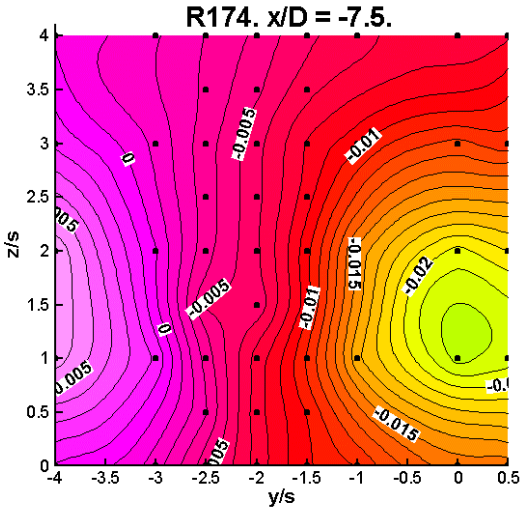

Figure 11. DW aircraft $\Delta C_T/\sigma$ as a function of UW aircraft position. Without ground plane. μ =0.10. DW C_T/σ (initial)=0.018; UW C_T/σ=0.12.

the aircraft separation distance increases. Without the ground plane (Fig. 11), the location of the peak remains essentially unchanged as the separation distance increases.

Flow visualization of tandem operations near the ground

In order to better understand the influence of the ground plane on the trailing wake of the upwind aircraft, two simple flow visualization techniques were implemented. First, a mixture consisting of motor oil, mineral spirits, olive oil, and red pigment was applied to the ground plane surface. The test conditions and upwind aircraft location corresponding to the peak negative C_{Mx}/σ shown in Fig. 8 were selected. The upstream aircraft was located at x/D=-2.5, y/s=-2.5, and z/s=1. A stable oil pattern developed after remaining on condition for approximately 20 minutes. Figure 12 shows the resulting oil pattern. Examination of the oil pattern at the ground plane leading edge indicated the presence of a laminar separation bubble followed by turbulent reattachment. Therefore, the boundary layer of the ground plane can be considered turbulent from the ground plane leading edge. The impingement of the upwind aircraft wake on the ground plane is clearly seen as a scoured region. The upwind right rotor wake is pointing directly towards the right downwind rotor. The upwind right rotor wake produces an upwash at the right downwind rotor, causing a negative rolling moment. Recall that without the ground plane (Fig. 9), the upwind right rotor wake is assumed to cause a downwash at the downwind left rotor.

Tufts were also used to provide qualitative information on the flow behavior. The tufts were attached in a 48x64 rectangular grid over the entire ground plane. The tufts were spaced 1 inch apart across the width of the ground plane and every 1.5 inches along the length of the ground plane. Each tuft had an active length of approximately 1 inch. The tufts were made of black acrylic yarn and were attached to the ground plane using 0.5-inch wide white electrical tape. Figure 13 shows the tuft pattern corresponding to the oil pattern in Fig. 12. A rough outline encompassing the tufts that are no longer pointing streamwise is shown superimposed on the tuft pattern in Fig. 13. The tuft pattern is qualitatively very similar to the oil pattern. Figure 14 shows the tuft pattern for test conditions corresponding to the peak positive moment shown in Fig. 8. The wake from the upwind right rotor is outboard of the downwind right rotor. This appears to cause a downwash on the right downwind rotor and a positive rolling moment. During the experiment, some of the tufts upstream of the upwind aircraft were observed to be vertical, indicating the presence of a ground vortex. The ground vortex is caused by the rotor outwash impinging on the ground plane and mixing

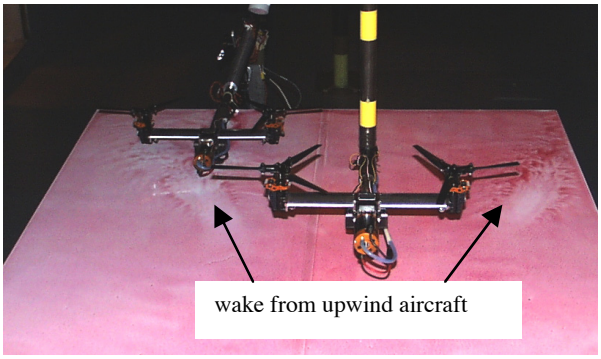

Figure 12. Oil pattern on ground plane.
Conditions: x/D=-2.5; y/s=-2.5; z/s=1; μ =0.10.
DW C_T/σ (initial)=0.019; UW C_T/σ=0.12.
View looking downstream.

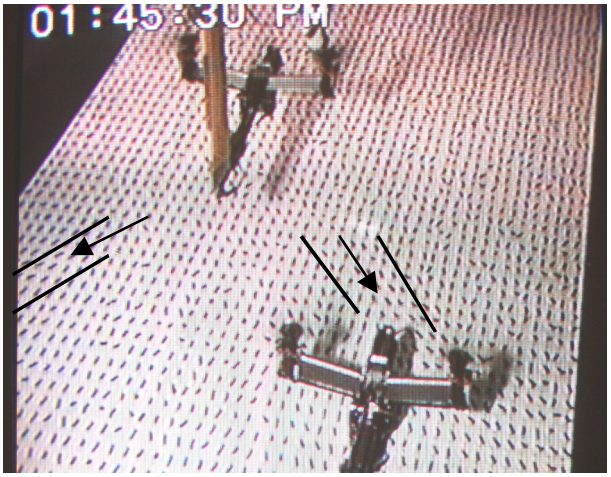

Figure 13. Tuft pattern on ground plane.
Conditions: x/D=-2.5; y/s=-2.5; z/s=1; μ=0.10;
DW C_T/σ (initial)=0.018; UW C_T/σ=0.12.
View looking upstream.

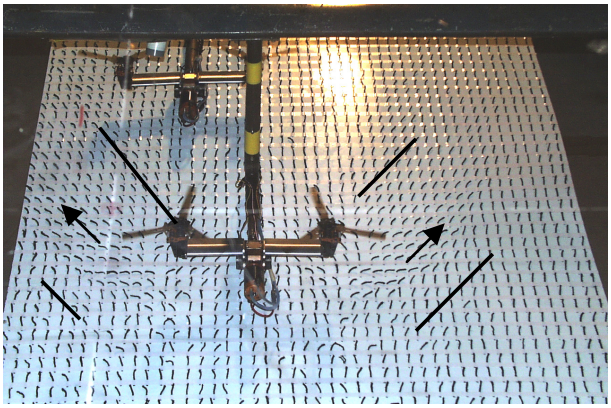

Figure 14. Tuft pattern on ground plane. Conditions: x/D=-2.5; y/s=-1; z/s=0.1; μ =0.10; DW C_T/σ(initial)=0.018; UW C_T/σ=0.121. View looking downstream.

with the oncoming freestream velocity. The wake of the upwind aircraft is affected not only by the ground plane, but also by the downwind aircraft whose own wake is spreading and forcing the upwind wake to spread out even further.

Clearly, the wake interactions interpreted from the flow visualization images are intriguing and complicated. Velocity field measurements in several cross-flow planes between the aircraft are required to truly understand the interaction of the aircraft wakes with the ground plane.

Scenario 3: Single Tiltrotor Operating in Winds Above Ground.

The effect of winds on a tiltrotor operating near the ground was next examined. For this scenario, the upwind aircraft was located at y/s=-1.72 (lateral mid-point of the ground plane) and x/D=-5. The downwind aircraft remained unpowered. At z/s=4, the upwind aircraft rpm was set to the design speed and the tunnel speed was increased to μ=0.10. The aircraft C_T/σ was set to 0.12 and the rolling moment was trimmed to approximately zero. From this point on, the controls remained fixed and the trim was allowed to vary. The upwind aircraft was then traversed from z/s=4 to slightly above the ground plane and then back to z/s=4. Tunnel speed was adjusted to the next desired μ and the height sweep was repeated. Figure 15 shows the results from height sweeps at μ=0, 0.05, and 0.10 (note μ=0.10 corresponds to 46 kts full-scale). As the winds increase, the rotor wakes are blown back and the effect of the ground plane on the aircraft thrust diminishes. In hover, there is a nearly 19% augmentation in thrust caused by the ground plane.

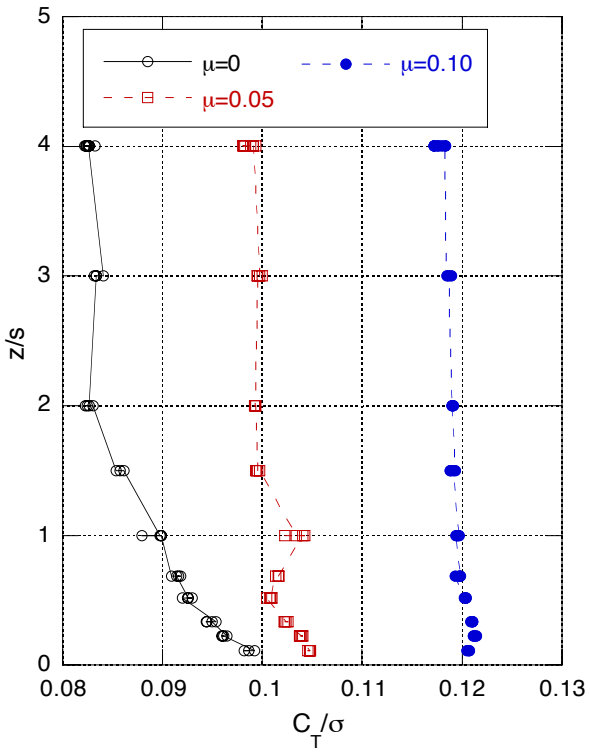

Figure 15. Ground effect on UW aircraft thrust. x/D=-5; y/s=-1.72. UW C_T/σ (initial)=0.12; DW rpm=0.

Conclusions

Three scenarios representing tandem level flight, tandem operations near the ground, and a single tiltrotor operating above the ground for varying winds are examined. The results from this experiment have provided significant insight into the aerodynamic interaction of two tiltrotors in helicopter-mode operating in close proximity to each other with and without a ground plane. These data provide guidance on determining tiltrotor flight formation configurations that minimize disturbance to the following aircraft. Key findings are listed below.

Scenario 1: Level Flight

1. Peak rolling moments occur on the downwind aircraft when the upwind aircraft right (left) rotor is laterally aligned with the downwind left (right) rotor for aircraft separation distances of x/D=-2.5 to –10.
2. Peak reductions in thrust occur when the two aircraft centerlines are aligned laterally. The magnitude decreased slightly with increasing streamwise aircraft separation distance.
3. For fixed advance ratio, the peak rolling moment on the downwind aircraft decreased slightly as the streamwise separation distance between the two aircraft increased from x/D= -2.5 to -10.
4. The magnitude of the peak roll moment was more sensitive to changes in the upwind aircraft thrust at the lower advance ratio of 0.05 compared with 0.10.
5. The differential collective pitch required to trim the peak negative rolling moment was estimated using a thrust derivative derived from isolated tiltrotor data. The estimate compared well with the value predicted by CAMRAD II.

Scenario 2: Tandem Operations Near the Ground

6. The ground plane forces the aircraft wakes to spread laterally. As a result, the downwind aircraft peak roll moment occurs with the upwind aircraft further outboard of the

downwind aircraft compared to the case without the ground plane.

7. The magnitudes of the peak roll moment and thrust change decrease with increasing aircraft streamwise separation distance.

Scenario 3: Single Tiltrotor Operating in Winds Above Ground.

8. The ground plane causes an increase in thrust as the aircraft height above the ground plane decreases. The thrust increase diminishes as the forward speed increases.

Acknowledgements

The authors wish to thank Mark Betzina and Wayne Johnson of NASA Ames for their helpful discussions on estimating differential collective pitch. In addition, the support from the test crew at the U. S. Army 7- by 10-Foot Wind Tunnel is gratefully acknowledged.

References

1. Abrego, A. I., Betzina, M. D., and Long, K. L., "A Small-Scale Tiltrotor Model Operating in Descending Flight," 28th European Rotorcraft Forum, Bristol, United Kingdom, September 2002.
2. Betzina, M. D., "Tiltrotor Descent Aerodynamics: A Small-Scale Experimental Investigation of Vortex Ring State," American Helicopter Society 57th Annual Forum, Washington, D. C., May 2001.
3. Johnson, W., Yamauchi, G. K., Derby, M. D., and Wadcock, A. J., "Wind Tunnel Measurements and Calculations of Aerodynamic Interactions Between Tiltrotor Aircraft," American Institute of Aeronautics and Astronautics, 41st Aerospace Sciences Meeting and Exhibit, Reno, NV, January 2003.
4. Derby, M. D. and Yamauchi, G. K., "Design of 1/48th-Scale Models for Ship/Rotorcraft Interaction Studies," AIAA-2003-3952, 21st AIAA Applied Aerodynamics Conference, Orlando, FL, June 2003.
5. Blake, W. and Multhopp, D., "Design, Performance and Modeling Considerations For Close Formation Flight," AIAA-98-4343, August 1998.
6. Blake, W., "Drag Reduction from Formation Flight," Air Force Research Laboratory Technology Horizons, December 2002.
7. Ray, R. J., Cobleigh, B. R., Vachon, M. J., and St. John, C., "Flight Test Techniques Used to Evaluate Performance Benefits During Formation Flight," AIAA-2002-4492, AIAA Atmospheric Flight Mechanics Conference and Exhibit, Monterey, CA, August 2002.
8. Felker, F. F., Signor, D. B., Young, L. A., and Betzina, M. D., "Performance and Loads Data From a Hover Test of a 0.658-Scale V-22 Rotor and Wing," NASA TM 89419, April 1987.
9. Felker, F. F., Betzina, M. D., and Signor, D. B., "Performance and Loads Data from a Hover Test of a Full-Scale XV-15 Rotor," NASA TM 86833, November 1985.
10. Betzina, M. D., "Rotor Performance of an Isolated Full-Scale XV-15 Tiltrotor in Helicopter Mode," American Helicopter Society Aerodynamics, Acoustics, and Test and Evaluation Technical Specialists Meeting, San Francisco, CA, January 2002.
11. Johnson, W., "Influence of Wake Models on Calculated Tiltrotor Aerodynamics," American Helicopter Society Aerodynamics, Acoustics, and Test and Evaluation Technical Specialists Meeting, San Francisco, CA, January 2002.
12. Branum, L. and Tung, C., "Performance and Pressure Data from a Small Model Tilt-Rotor in Hover," NASA TM 110441, USAATCOM TR 97-A-003, April 1997.

.